

Pattern formation within *Escherichia coli*: diffusion, membrane attachment, and self-interaction of MinD molecules

Rahul V. Kulkarni^{1,*}, Kerwyn Casey Huang^{1,2,†}, Morten Kloster¹, and Ned S. Wingreen^{1,3}

¹NEC Laboratories America, Inc., Princeton, New Jersey 08540

²Department of Physics, Massachusetts Institute of Technology, Cambridge, Massachusetts 02139 and

³ Department of Molecular Biology, Princeton University, Princeton, New Jersey 08540

(Dated: October 29, 2018)

In *E. coli*, accurate cell division depends upon the oscillation of Min proteins from pole to pole. We provide a model for the polar localization of MinD based only on diffusion, a delay for nucleotide exchange, and different rates of attachment to the bare membrane and the occupied membrane. We derive analytically the probability density, and correspondingly the length scale, for MinD attachment zones. Our simple analytical model illustrates the processes giving rise to the observed localization of cellular MinD zones.

PACS numbers: 87.17.Ee, 87.16.Ac, 82.39.Rt

Understanding how proteins are directed to specific locations within the cell is one of the key challenges of cellular biology. At the basic level, targeting of proteins to subcellular locations is governed by *physical processes*. A striking example is the system of Min proteins, which functions as an internal spatial oscillator in *E. coli*, and is necessary for accurate cell division [1]. The properties and interactions of the three Min proteins, MinC, D, and E, have been revealed by recent experiments [2–11]. MinD is an ATPase—a protein which binds and hydrolyzes the nucleotide ATP to ADP. In its ATP-bound form, MinD associates with the inner membrane of the cell [7, 8], where it recruits cytoplasmic MinC [6] and MinE [7] onto the membrane. Once on the membrane, MinE activates hydrolysis of ATP by MinD which results in MinD dissociating from the membrane. MinE and MinD together produce a spatial oscillator with a period of ~ 40 seconds [7–10]. In each oscillation period, the majority of MinD molecules accumulate at one end of the cell forming a “polar zone”. The MinD polar zone then shrinks toward the end of the cell and a new MinD polar zone forms at the opposite pole. MinE is observed to form a ring at the medial edge of the MinD polar zone [12]. The MinE ring moves along with the polar zone edge as the MinD polar zone shrinks toward the end of the cell. The dynamics of MinC follows that of MinD [13]. Complexes of MinC and MinD on the membrane block the formation of a ring of FtsZ protein [4], a necessary first step in determining the site of cell division [5]. The spatial oscillations of MinD and MinC from pole to pole thus ensure that an FtsZ ring does not form near the poles, so that cell division can only occur near midcell. Recently, several numerical models have been proposed to explain the oscillatory behavior and mechanisms of protein targeting [14–19].

One of the key emergent properties of the Min oscillations is the length scale for formation of a new MinD attachment zone. In filamentous cells (*i.e.* cells that grow but do not divide), several MinD zones are observed in

a striped pattern with a characteristic length separating MinD attachment zones [8, 20]. In this Letter, we study the processes giving rise to new MinD attachment zones in the cell. Using a simple model, we demonstrate analytically that the length separating MinD zones depends on (*i*) the cytoplasmic diffusion coefficient and the nucleotide-exchange rate of MinD, and (*ii*) the rate of attachment of ATP-bound MinD to the membrane.

Model. Our aim is to illustrate the physical processes of reaction and diffusion that give rise to preferred length scales in the Min-protein system. Our 1D model for these processes is abstracted from the 3D numerical model of Ref. [18], which is based on measured properties of MinD and MinE and which reproduces the observed pattern in filamentous cells. Other models have also accounted for the oscillations of the Min proteins [14–16], including the striped pattern seen in filamentous cells. We begin by considering a fully formed “old” polar zone of ATP-bound MinD (MinD:ATP) in one half of the cell. MinE activates the ATPase activity of MinD, giving rise to a source of cytoplasmic MinD:ADP. Subsequently, there are two stages leading up to reattachment of MinD to the membrane: (*i*) diffusion of each MinD:ADP until nucleotide exchange transforms it into MinD:ATP, and (*ii*) continued diffusion of the MinD:ATP until it attaches to the membrane (see inset to Fig. 1). The attachment rate of MinD:ATP increases with the local concentration of membrane-bound MinD; thus the old polar zone is much stickier than the bare membrane [18]. Our aim is to derive analytically the density of attachment $\rho(x)$ of MinD:ATP outside the old polar zone, in order to obtain the length scale of the new MinD attachment zone.

Filamentous cell, single source. We approximate a long, filamentous cell as an infinite 1D line. The old polar zone of MinD occupies $x < 0$, and bare membrane occupies $x > 0$ (see inset to Fig. 1). To model the effect of the MinE ring at the edge of the MinD polar zone, we first consider that MinD:ADP dissociates from the membrane only at $x = 0$. After stage (*i*) – diffusion of

MinD:ADP until nucleotide exchange – the probability density of each MinD:ATP is

$$P_1(x) = \int_0^\infty P_D(x|t)Q_1(t)dt, \quad (1)$$

where $Q_1(t)$ is the waiting-time distribution for single-step nucleotide exchange with average waiting time τ_1 ,

$$Q_1(t) = \frac{1}{\tau_1} e^{-t/\tau_1}, \quad (2)$$

and $P_D(x|t)$ is the distribution following diffusion in 1D for time t with diffusion coefficient \mathcal{D} ,

$$P_D(x|t) = \frac{1}{\sqrt{4\pi\mathcal{D}t}} \exp\left(-\frac{x^2}{4\mathcal{D}t}\right). \quad (3)$$

Substituting Eqs. 2 and 3 into Eq. 1 yields the initial distribution of MinD:ATP in the cytoplasm

$$P_1(x) = \frac{1}{2\sqrt{\mathcal{D}\tau_1}} \exp\left(-\sqrt{\frac{x^2}{\mathcal{D}\tau_1}}\right). \quad (4)$$

During stage (ii)—diffusion of MinD:ATP until membrane reattachment—we initially assume that the region of the old polar zone ($x < 0$) is infinitely sticky for MinD:ATP. Hence, if a MinD:ATP diffuses into $x < 0$, it will immediately reattach and become part of the old polar zone. Thus only those MinD:ATP molecules formed at $x > 0$ which *never* cross the origin in the course of cytoplasmic diffusion will attach to form the new zone. Given an initial position $x_0 > 0$ of a MinD:ATP, the probability that it diffuses to some $x > 0$ after time t is $P_D(x-x_0|t)$. We define the probability that a MinD:ATP diffuses to some $x > 0$ after time t *without crossing* $x = 0$ by $P_2(x, x_0|t)$. The probability distribution $P_2(x, x_0|t)$ can be calculated using the continuum version of the Reflection Principle [21],

$$P_2(x, x_0|t) = P_D(x - x_0|t) - P_D(x + x_0|t). \quad (5)$$

The attachment density $\rho(x)$ for the bare membrane at $x > 0$ can now be obtained from

$$\rho(x) = \int_0^\infty dx_0 \int_0^\infty dt P_2(x, x_0|t) P_1(x_0) Q_2(t), \quad (6)$$

where $Q_2(t) = (1/\tau_2) \exp(-t/\tau_2)$ is the distribution of waiting times for membrane attachment with average waiting time τ_2 . Integrating over t and x_0 in Eq. 6, we obtain (for $\tau_1 \neq \tau_2$)

$$\rho(x) = \frac{p_{\text{tot}}}{\sqrt{\mathcal{D}\tau_1} - \sqrt{\mathcal{D}\tau_2}} \left(e^{-x/\sqrt{\mathcal{D}\tau_1}} - e^{-x/\sqrt{\mathcal{D}\tau_2}} \right), \quad (7)$$

where the total probability of attachment to the bare membrane at $x > 0$ is

$$p_{\text{tot}} = \frac{\sqrt{\tau_1}}{2(\sqrt{\tau_1} + \sqrt{\tau_2})}. \quad (8)$$

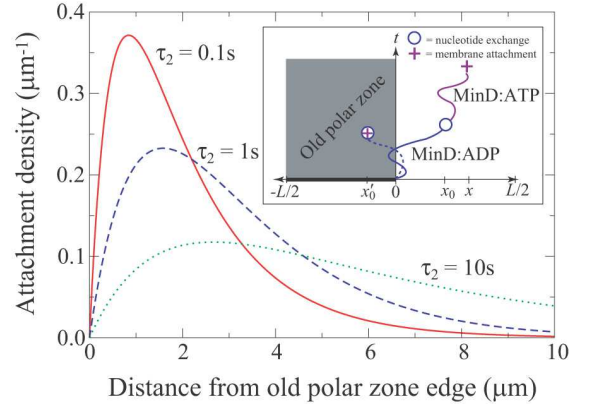


FIG. 1: (Color online) Normalized attachment density $\rho(x)/p_{\text{tot}}$ (Eq. 7) for different average attachment waiting times τ_2 from 0.1s to 10s, with the diffusion coefficient $\mathcal{D} = 2.5 \mu\text{m}^2/\text{s}$ and average nucleotide-exchange waiting time $\tau_1 = 1\text{s}$ taken from Ref. [18]. Inset: cartoon of attachment processes. The solid blue line shows a MinD:ADP which diffuses to the position x_0 before undergoing nucleotide exchange. The resulting MinD:ATP then continues to diffuse until it attaches to the bare membrane at x , without ever crossing the edge of the old polar zone at $x = 0$. In contrast, the dashed blue line shows a MinD:ADP which undergoes nucleotide exchange at the position x_0' , where it immediately reattaches to the membrane in the old polar zone.

In the limit $\tau_2 \rightarrow 0$, where the membrane is everywhere perfectly sticky for MinD:ATP, Eq. 8 gives $p_{\text{tot}} = 1/2$, as required by symmetry. In the opposite limit, $\tau_2 \gg \tau_1$, where sticking of MinD:ATP to the bare membrane at $x > 0$ is slow, only a small fraction, $p_{\text{tot}} = \sqrt{\tau_1/4\tau_2}$, attach to the bare membrane.

We expect that polymerization of MinD:ATP on the membrane leads to autocatalytic membrane attachment that enhances the peak in the attachment density [18]. Thus, the relevant length scale to characterize the new MinD:ATP zone is the position of the maximum in $\rho(x)$, which occurs at

$$x_{\text{max}} = \frac{\sqrt{\mathcal{D}\tau_1\tau_2}}{2(\sqrt{\tau_2} - \sqrt{\tau_1})} \log\left(\frac{\tau_2}{\tau_1}\right). \quad (9)$$

In Fig. 1, we plot the normalized MinD:ATP attachment density $\rho(x)/p_{\text{tot}}$ from Eq. 7. At large distances, the profile decays exponentially as expected for a diffusive process (see Eq. 4). However, for a simple diffusive process we expect the profile to have a maximum at the source position, *i.e.*, at $x = 0$. In contrast, we find that the probability of attachment is *zero* at the edge of the old polar zone at $x = 0$. This “zero boundary condition” follows from the infinite stickiness of the old polar zone for MinD:ATP. Any MinD:ATP which forms near the old polar zone has a high probability of crossing into $x < 0$ and immediately reattaching as part of the old polar zone. Only those MinD:ATP which form sufficiently far from

the old polar zone are likely to reattach as part of the new MinD:ATP attachment zone. The two competing effects, the zero boundary condition at $x = 0$ and the exponential decay due to diffusion as indicated in Eq. 4, set the length scale for the formation of the new MinD:ATP attachment zone. In the model from Ref. [18], the time scale for sticking to a bare membrane is $\tau_2 \sim 10$ s, giving $x_{\max} = 2.7\mu\text{m}$. This length scale agrees qualitatively with half the center-to-center distance ($\sim 3\mu\text{m}$) between neighboring MinD attachment zones as observed in Ref. [8].

Filamentous cell, distributed source. In the preceding analysis, the polar-zone edge at $x = 0$ was taken to be the only source of MinD:ADP. However, in experiments some MinE is observed throughout the MinD polar zone [11, 12], suggesting that cytoplasmic MinD:ADP is released throughout the old polar zone as well. What effect, if any, does this have on the length scale for formation of the new MinD attachment zone? Instead of assuming a single source for MinD:ADP at $x = 0$, we now consider a source with distribution $w(x_s)$, $x_s \leq 0$. This distributed source of MinD:ADP modifies Eq. 1:

$$P_1(x) \rightarrow \int_0^\infty dt \int_{-\infty}^0 dx_s w(x_s) P_D(x - x_s|t) Q_1(t), \quad (10)$$

where x_s describes the position of the MinD:ADP when it leaves the membrane. Integrating over t , we find for $x > 0$,

$$P_1(x) = \frac{1}{2\sqrt{\mathcal{D}\tau_1}} e^{-x/\sqrt{\mathcal{D}\tau_1}} \left[\int_{-\infty}^0 dx_s w(x_s) e^{x_s/\sqrt{\mathcal{D}\tau_1}} \right]. \quad (11)$$

Comparing to Eq. 4, we see that a distributed source of MinD:ATP simply reduces $P_1(x)$ by the constant factor in square brackets. Therefore, the attachment density is the same as in Eq. 7, with p_{tot} reduced by the constant factor in square brackets. This leaves x_{\max} unchanged, so the length scale for formation of the new MinD attachment zone is identical.

Finite polar-zone attachment probability. How is the reattachment profile altered by relaxing the approximation that the old polar zone is infinitely sticky for MinD:ATP? To treat the case where the mean attachment time to the old polar zone is $\tau_3 > 0$, we introduce the quantities $\rho_c(x, t)$ and $\rho_m(x, t)$, respectively denoting the densities of cytoplasmic- and membrane-bound MinD:ATP as functions of time. Our previous expression for the membrane attachment density $\rho(x)$ (Eq. 7) is then equivalent to $\rho_m(x, t \rightarrow \infty)$ for the case $\tau_3 = 0$ and $x > 0$.

The time-dependent densities of MinD in the cytoplasm and on the membrane are described by the fol-

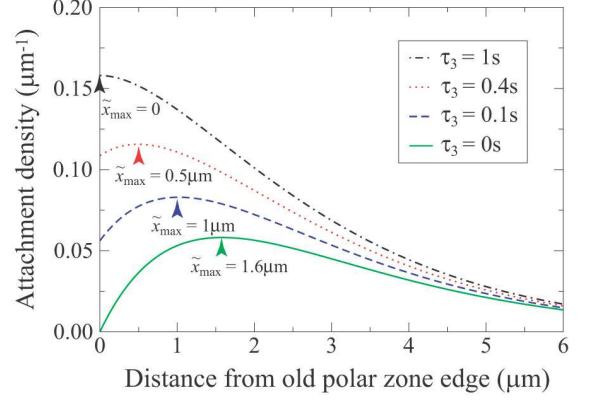


FIG. 2: (Color online) Attachment density $\tilde{\rho}(x)$ (Eq. 16) for different values of τ_3 , the average attachment time of MinD:ATP in the old polar zone, with $\mathcal{D} = 2.5\mu\text{m}^2/\text{s}$, average nucleotide exchange waiting time $\tau_1 = 1$ s, and average bare-membrane attachment time $\tau_2 = 1$ s. Note the shift of the maximum toward $x = 0$ as $\tau_3 \rightarrow \tau_2$.

lowing equations

$$\frac{\partial \rho_c(x, t)}{\partial t} = \mathcal{D} \frac{\partial^2 \rho_c(x, t)}{\partial x^2} - \frac{1}{\tau(x)} \rho_c(x, t) \quad (12)$$

$$\frac{\partial \rho_m(x, t)}{\partial t} = \frac{1}{\tau(x)} \rho_c(x, t) \quad (13)$$

where

$$\tau(x) = \begin{cases} \tau_2 & x > 0 \\ \tau_3 & x \leq 0 \end{cases} \quad (14)$$

We are interested in the final density of MinD on the membrane $\rho_m(x, t \rightarrow \infty)$ for $x > 0$, which, from integrating Eq. 13, is given by $\frac{1}{\tau_2} \int_0^\infty \rho_c(x, t) dt \equiv f(x)/\tau_2$. Similarly, we define $\rho_m(x, t \rightarrow \infty) \equiv f(x)/\tau_3$ for $x \leq 0$. Then the unknown function $f(x)$ satisfies

$$\rho_c(x, 0) = -\mathcal{D} \frac{d^2 f}{dx^2} + \frac{1}{\tau(x)} f(x). \quad (15)$$

Note that $\rho_c(x, 0)$ is the initial distribution of MinD:ATP in the cytoplasm, which is given by Eq. 4. We can now readily solve Eq. 15 for $f(x)$ in the regions $x \leq 0$ and $x > 0$, subject to the boundary conditions that $f(x)$ vanishes at $\pm\infty$ and is continuous and differentiable at $x = 0$.

The new MinD:ATP attachment profile for $x > 0$ with a finite binding rate $1/\tau_3$ in the old polar zone is

$$\tilde{\rho}(x) = \frac{f(x)}{\tau_2} = \frac{1}{2(\tau_1 - \tau_2)} \sqrt{\frac{1}{\mathcal{D}\tau_2}} \left(\sqrt{\tau_1\tau_2} e^{-x/\sqrt{\mathcal{D}\tau_1}} - \frac{2\tau_2\sqrt{\tau_1\tau_3} + 2\tau_2\tau_3 + \tau_1\tau_2 - \tau_1\tau_3}{(\sqrt{\tau_1} + \sqrt{\tau_3})(\sqrt{\tau_2} + \sqrt{\tau_3})} e^{-x/\sqrt{\mathcal{D}\tau_2}} \right). \quad (16)$$

In Fig. 2, we plot $\tilde{\rho}(x)$ for $\tau_2 = 1$ s and four values of τ_3 : 0s, 0.1s, 0.4s, and 1s. For $\tau_3 = 0$ s, the density profile

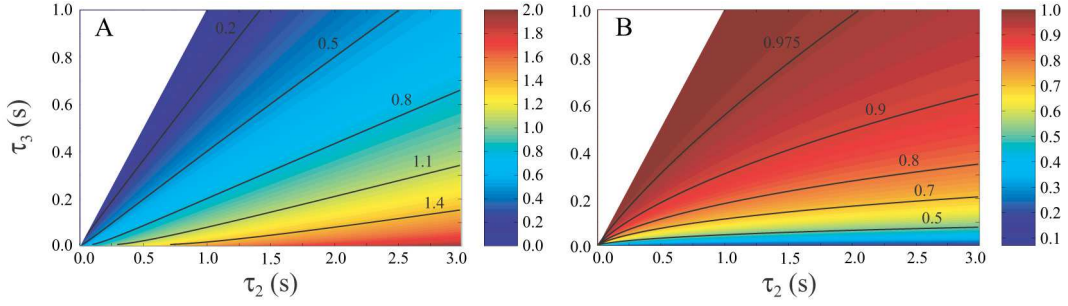


FIG. 3: (Color) (a) The position of the maximum in the MinD-attachment profile, \tilde{x}_{\max} (Eq. 17), as a function of $\tau_2 \in [0s, 3s]$ and $\tau_3 \in [0s, 1s]$. (b) The ratio of densities $f(0)/f(\tilde{x}_{\max})$.

in Eq. 7 is reproduced. For $\tau_3 = \tau_2 = 1s$, the profile is symmetric about $x = 0$ with a maximum at $x = 0$. The intermediate values show a shift in the maximum toward $x = 0$ as τ_3 approaches τ_2 , and a finite density at $x = 0$.

The maximum occurs at

$$\tilde{x}_{\max} = \frac{\sqrt{D\tau_1\tau_2}}{\sqrt{\tau_2} - \sqrt{\tau_1}} \log \left(\frac{\tau_2(\sqrt{\tau_1} + \sqrt{\tau_3})(\sqrt{\tau_2} + \sqrt{\tau_3})}{2\tau_2\sqrt{\tau_1\tau_3} + 2\tau_2\tau_3 - \tau_1\tau_3 + \tau_1\tau_2} \right), \quad (17)$$

which is less than x_{\max} (see Eq. 9) for all nonzero τ_3 . Another quantity of interest is the ratio of the MinD:ATP density at the polar-zone edge to the peak density, $\eta = f(0)/f(x_{\max})$. This is a measure of the spatial definition of the new polar zone. In Fig. 3, we plot (a) \tilde{x}_{\max} and (b) $f(0)/f(\tilde{x}_{\max})$ for $\tau_2 \in [0s, 3s]$ and $\tau_3 \in [0s, 1s]$, $\tau_3 < \tau_2$. Interestingly, except for very small τ_3 , \tilde{x}_{\max} is a function only of the ratio τ_2/τ_3 . Note also that the ratio η is small only for very low values of τ_3 . These results demonstrate that the asymmetry of binding probabilities to the old polar zone and to the bare membrane is crucial to establish a new attachment zone well separated from the old one.

In summary, we have studied the processes that give rise to the length scale observed in cellular MinD attachment zones. Our analysis indicates that this length scale is an emergent property of the system which depends primarily on (i) the rate of nucleotide exchange, (ii) the rates of membrane attachment, and (iii) the diffusion constant for MinD. It is important to note that these are biochemical properties of MinD which can be fine tuned by evolution. Our analysis suggests that these parameters are tuned to block minicelling at the cell poles and at the same time to permit cell division at the cell center. Finally, we note that the Min system serves as an example of how physical processes can produce subcellular protein localization. While MinD is “targeted” to the cell poles, the mechanism is not based on recruitment by a biological target, but rather on a dynamical physical instability in the system.

We thank Kevin Beach for valuable suggestions. Partial funding for this research was provided by the MRSEC

program of the NSF under grant number DMR-0213282.

* Electronic address: kulkarni@vt.edu; Present address: Department of Physics, Virginia Polytechnic and State University, Blacksburg, VA 24061

† Present address: Department of Molecular Biology, Princeton University, Princeton, New Jersey 08540

- [1] X.-C. Yu and W. Margolin, *Mol. Microbiol.* **32**, 315 (1999).
- [2] P. A. J. de Boer, R. E. Crossley, and L. I. Rothfield, *Cell* **56**, 641 (1989).
- [3] P. A. J. de Boer, R. E. Crossley, and L. I. Rothfield, *J. Bacteriol.* **174**, 63 (1992).
- [4] E. Bi and J. Lutkenhaus, *J. Bacteriol.* **175**, 1118 (1993).
- [5] E. Bi and J. Lutkenhaus, *Nature* **354**, 161 (1991).
- [6] J. Huang, C. Cao, and J. Lutkenhaus, *J. Bacteriol.* **178**, 5080 (1996).
- [7] Z. Hu, E. P. Gogol, and J. Lutkenhaus, *Proc. Nat. Acad. Sci. USA* **99**, 6761 (2002).
- [8] D. M. Raskin and P. A. J. de Boer, *Proc. Nat. Acad. Sci. USA* **96**, 4971 (1999).
- [9] Z. Hu and J. Lutkenhaus, *Mol. Microbiol.* **34**, 82 (1999).
- [10] X. Fu, Y.-L. Shih, Y. Zhang, and L. I. Rothfield, *Proc. Nat. Acad. Sci. USA* **98**, 980 (2001).
- [11] Y.-L. Shih, T. Le, and L. Rothfield, *Proc. Nat. Acad. Sci. USA* **100** (2003).
- [12] D. M. Raskin and P. A. J. de Boer, *Cell* **91**, 685 (1997).
- [13] D. M. Raskin and P. A. J. de Boer, *J. Bacteriol.* **181**, 6419 (1999).
- [14] M. Howard, A. D. Rutenberg, and S. de Vet, *Phys. Rev. Lett.* **87**, 278102 (2001).
- [15] H. Meinhardt and P. A. J. de Boer, *Proc. Nat. Acad. Sci. USA* **98**, 14202 (2001).
- [16] K. Kruse, *Biophys. J.* **82**, 618 (2002).
- [17] M. Howard and A. D. Rutenberg, *Phys. Rev. Lett.* **90**, 128102 (2003).
- [18] K. C. Huang, Y. Meir, and N. Wingreen, *Proc. Nat. Acad. Sci. USA* **100**, 12724 (2003).
- [19] M. Howard, *J. Mol. Biol.* **335**, 655 (2004).
- [20] C. A. Hale, H. Meinhardt, and P. A. J. de Boer, *EMBO J.* **20**, 1563 (2001).
- [21] W. Feller, *An Introduction to Probability Theory and Its Applications* (Wiley, New York, 1968), 3rd ed.